Vol 13 No 5, May 2004
1009-1963/2004/13(05)/0646-11

Chinese Physics

© 2004 Chin. Phys. Soc.
and IOP Publishing Ltd

The production of slow particles in ^{16}O–Em interactions at 4.5 A GeV/c*

Wu Feng-Juan(吴凤娟), Zhang Dong-Hai(张东海)†,
Li Jun-Sheng(李俊生), and Li Zhen-Yu(李振宇)

Institute of Modern Physics, Shanxi Normal University, Linfen 041004, *China*

(Received 10 June 2003; revised manuscript received 31 October 2003)

A sample of 1233 events is used to study the general characteristics of ^{16}O–Em interactions at 4.5 A GeV/c. Multiplicity and angular distributions of slow particles and correlations among them are discussed. The present data are compared with the corresponding results from the interactions of other projectiles at the same energy and also the same projectile at different energies. The results indicate that black particle production is independent of the energy and mass of the projectile, but for grey particles it is dependent on the mass of projectile.

Keywords: relativistic heavy-ion collision, slow particles, multiplicity distribution, angular distribution, multiplicity correlation

PACC: 2570N, 2320E, 2940R

1. Introduction

The study of relativistic high-energy nucleus–nucleus reactions has become an extremely interesting subject for physicists working in nuclear physics, particle physics, and statistical physics. This is perhaps due to the fact that such heavy-ion interactions may provide us with nuclear matter at an extremely high density and temperature so as to reveal many new phenomena.[1–3] One of such phenomena predicted by theorists is the phase transition of hadron gas to quark–gluon plasma (QGP).[4] It has been suggested that relativistic heavy-ion collisions present a possible way to study extended matter in the laboratory under extremes of energy density otherwise available only in the hot early universe, or in certain astrophysical situation of strong gravitational collapse. It is hoped that such collisions can possibly create regions of deconfined matter so energetic that the normal forces that confine quarks and gluons into individual hadrons are overcome and the matter in the interaction region is in the form of an extended QGP. However, the first goal for such studies is to investigate how favourable the experimental conditions are for a phase transition from hadronic matter to QGP. To detect this abnormal nuclear phenomenon, first the normal nuclear collision mechanism has to be understood.

As in collisions of hadrons with nucleon and nuclei, a large part of the total cross section for nucleus–nucleus collisions at high energies is due to the multiple production of particles. Thus, for understanding the normal collision mechanism, measurements on the multiplicities of charged secondaries, multiplicity correlations between various multiplicity parameters, angular distribution of different particles, etc., are needed. Thus, it is considered worthwhile to study the normal collision mechanism in more detail.

The results from experiments in recent years on ultrarelativistic heavy-ion collisions indicate the importance of rescattering and cascading of nuclear constituents. The spectator parts, which do not interact in the initial stage of the collision, play however an important role in later evolution of the collisions. Models that are quite successful in explaining the particle production in the central rapidity region normally fail when describing the particle yields in the fragmenta-

*Project supported by the National Natural Science Foundation of China (Grant No 10275042), the Shanxi Provincial Natural Science Foundation (Grant No 20021007) and Shanxi Provincial Foundation for Returnees.

†E-mail: zhangdh@dns.sxtu.edu.cn

tion regions, unless additional assumptions about the later stages of the collisions are made. In the target fragmentation region grey and black particles are produced. From studies of grey particles in hadron–nucleus and recently also in nucleus–nucleus interactions [5] we have learned that their features are essentially energy independent and that they are to a large extent governed by the nuclear geometry. In hadron-induced interactions grey particles are indeed used as a direct measure of the number of participating target nucleons.[6,7] Experimentally, a large fraction of the grey particles are protons knocked out of the target, and are thus directly probing the rescattering. The emission of the black particles has been well explained in terms of the statistical evaporation model where complete thermalization is believed to occur in the final stages of reaction. For a better understanding of the production mechanism of target fragments, more and detailed experimental results are needed. In the present work, an attempt has been made to study the characteristics of slow particles, such as the multiplicity distributions of grey and black particles, their dispersion, and multiplicity correlations among various charged secondaries produced in 4.5 A GeV/c ^{16}O–nucleus interactions.

2. Experimental details

NIKFI BR-2 stacks of nuclear emulsions, 10cm× 10cm×2cm in volume, were exposed horizontally to the 4.5 A GeV/c ^{16}O beam at Synchro-phasotron of the Joint Institute of Nuclear Research (JINR), Dubna. The flux intensity was 10^3 particles/cm^2. Emulsion plates, 600μm in thickness, were scanned by the along-the-track method using XSJ-1 and XSJ-2 microscopes under 100× oil objectives and 16× eyepieces. The tracks were picked up at a distance of 1cm from the edge of the pellicles and were carefully followed until they either interacted with the nuclei of emulsion or escaped from the pellicle. A total of 2292 interactions of oxygen were observed by following 28390.4cm of primary track length, leading to the mean free path $\lambda = (12.39 \pm 0.26)$cm. Among these interactions 111 events were found to be produced by electromagnetic interactions and 109 events were due to elastic interactions. Out of these, 1233 interactions were picked up, without any bias, for the final analysis. Interactions which were within 30μm from the top or bottom surface of the emulsion were not considered for the final analysis.

The tracks of the emitted secondary charged particles in each interaction were classified, in accordance with emulsion terminology, into the following types:

(a) Shower tracks N_s correspond to the produced single-charged relativistic particles having velocity $\beta \geq 0.7$. Most of these tracks belong to pions contaminated with small proportions of fast protons and K mesons. Their multiplicity is denoted by n_s(not including the stripped projectile protons).

(b) Grey tracks N_g, with a range in emulsion $L >$ 3mm and velocity $0.3 < \beta < 0.7$, are mostly recoil protons in the kinetic energy range $26 \leq E \leq 375$MeV and a few kaons of kinetic energies $20 \leq E \leq 198$MeV and pions with kinetic energies of $12 \leq E \leq 56$MeV. The corresponding multiplicity of these grey tracks is denoted by n_g.

(c) Black tracks N_b, with a range in emulsion $L \leq$ 3mm and $\beta < 0.3$, correspond to protons with kinetic energies $E \leq 26$MeV, produced by low-energy target fragments. Their multiplicity is denoted by n_b.

The grey and black tracks together are called heavy ionizing particles. Their multiplicity is denoted by $n_h = n_g + n_b$.

(d) Projectile fragments (PFs) N_f, a charged particle emitted at an angle $\theta \leq \Theta_f$ (Θ_f is the projectile fragmentation angle), without change in its ionization for at least 2cm from the interaction point, is considered as a noninteracting projectile fragment. The fragmentation angle is defined as $\Theta_f = p_f/p_{beam}$, where, p_{beam} stands for the beam momentum and p_f for the Fermi momentum of the nucleon; the latter is estimated to be 200 MeV/c, thus giving $\Theta_f \approx 45$mrad for the present incident energy. The charges of the projectile spectators are identified by the delta-ray-counting method.[8]

The characteristic features of nucleus–nucleus interactions at relativistic energies depend, from the geometrical point of view, on the impact parameter. The type of interaction is determined by the value of impact $b = (R_p + R_T)$ for peripheral interactions, $|R_p - R_T| \leq b < (R_p + R_T)$ for semi-central interactions and $b < |R_p - R_T|$ for central interactions, where R_p and R_T are the radii of the projectile and target. In peripheral interactions the colliding nuclei are well separated in their centra. This allows only a small momentum transfer between the nuclei, leading to the break-up of one or both of them into fragments. The characteristics of the emitted fragments are determined by the intrinsic Fermi momentum distribution of nucleons within the fragmenting nuclei.[9] The

projectile fragments are emitted within a narrow cone around the beam direction, while the target fragments are nearly isotropically distributed in the laboratory frame. Peripheral events are events with PFs of charge $Z \geq 2$ emitted in the forward core; these events show considerably less involvement of the projectile nucleus since they are formed at relatively large values of b. Central interactions are events which exhibit no PFs with charge $Z \geq 2$ in the forward core. Such events are thought to be produced by a violent destruction of the projectile and target nuclei at small values of the impact parameter of collision.

3. Experimental results

3.1. Target identification

Although the exact identification of target in an emulsion experiment is not easy as the medium is composed of H, C, N, O, Ag, Br and I nuclei, statistically the classification of interaction with different target nuclei in the emulsion could be done on the basis of the distribution of heavy particles, N_h, which is a characteristic of the size of the target. The events with $N_h \leq 1$ are collisions with hydrogen (^{16}O-H, A_T=1), the events with $1 < N_h \leq 7$ are collisions with light nuclei (^{16}O–CNO, $< A_T >= 14$) and the events with $N_h > 7$ are collisions with heavy nuclei (^{16}O–AgBr, $< A_T >= 94$). For the events with $1 < N_h \leq 7$ there are some admixture of peripheral ^{16}O–AgBr interactions. In Table 1 we present the percentage of different kinds of interactions induced by various projectiles in the emulsion.

Table 1. Percentage of occurrence of interactions for different groups of nuclei in emulsion.

Momentum /(A GeV/c)	Projectile	H	CNO	AgBr	Ref.
4.5	^{1}H	23.60	38.70	37.81	[10]
4.5	^{4}He	21.03	40.42	38.55	[11]
4.5	^{12}C	21.39	30.87	47.84	[12]
4.5	^{16}O	17.68	39.66	42.66	This work
4.5	^{28}Si	22.23	24.43	53.34	[13]

3.2. Multiplicity distributions of slow particles

Table 2 presents the mean multiplicity of black, grey and heavy ionizing particles from ^{16}O–Em interactions. In the table we also presents some similar results from the interaction of various projectiles with the emulsion. It can be seen from the table that $< N_b >$ remains practically unchanged from proton to silicon, indicating the approximate equality of the residual nucleus excitations. A comparison of the data presented in the table shows that $< N_g >$ increases with the mass of the projectile. This can be understood in terms of a participant–spectator picture of collision if we assume that the particles producing grey tracks come from the participant domain. The number of participant nucleon increases as the overlap volume of the target and the projectile increases. This volume is large for heavier beam nuclei, resulting in a larger value of $< N_g >$. Figure 1 shows the multiplicity distributions of grey, black and heavy ionizing particles from ^{16}O–Em interactions at 3.7 A GeV, 60 A GeV [25] and 200 A GeV [26] together with those from p–Em,[10] ^{4}He–Em,[11] ^{12}C–Em and ^{28}Si–Em at 4.5 A GeV/c.[18] From the figure it follows that

Table 2. Values of $< N_b >$, $< N_g >$, and $< N_h >$ in p–nucleus and nucleus–nucleus reactions at 4.5 A GeV/c.

Projectile	$< N_b >$	$< N_g >$	$< N_h >$	Ref.
^{1}H	3.77 ± 0.08	2.81 ± 0.06	6.58 ± 0.12	[14]
^{4}He	4.70 ± 0.20	4.70 ± 0.20		[11]
^{6}Li	5.35 ± 0.16	4.47 ± 0.16		[15]
^{12}C	4.49 ± 0.24	5.93 ± 0.34		[13]
^{12}C	4.38 ± 0.16	6.20 ± 0.14	10.58 ± 0.13	[14]
^{12}C	4.51 ± 0.10	5.96 ± 0.13		[16]
^{12}C	4.39 ± 0.09	5.98 ± 0.13	10.39 ± 0.16	[17]
^{12}C	4.51 ± 0.09	5.75 ± 0.11		[18]
^{16}O	4.88 ± 0.29	7.60 ± 0.60		[19]
^{16}O	5.38 ± 0.15	4.80 ± 0.17	10.18 ± 0.29	This work
^{22}Ne	4.22 ± 0.03	6.32 ± 0.04		[20]
^{24}Mg	7.70 ± 0.15	12.29 ± 0.20	19.99 ± 0.43	[14]
^{24}Mg	5.31 ± 0.17	7.85 ± 0.29		[21]
^{24}Mg	5.32 ± 0.13	7.88 ± 0.21	12.58 ± 0.31	[22]
^{28}Si	4.69 ± 0.23	8.59 ± 0.26	13.28 ± 0.41	[13]
^{28}Si	5.98 ± 0.31	8.26 ± 0.22	14.24 ± 0.48	[23]
^{28}Si	5.26 ± 0.09	6.33 ± 0.10		[18]
^{28}Si	4.82 ± 0.14	6.75 ± 0.24		[24]

(1) For the same projectile at different energies, the multiplicity distributions of target fragments (N_g, N_b and N_h) follow the same trend (Figs.1(a)–(c)). The percentages of events showing no sign of target fragmentation (white stars, $N_h = 0$) are 8.8, 14.6 and 18.3% respectively, for ^{16}O at 3.7, 60 and 200 A GeV, which indicate that the number of white stars increases with the increase of beam energy. There is a peak at $N_h = 4$ which is the contribution of light targets (CNO).

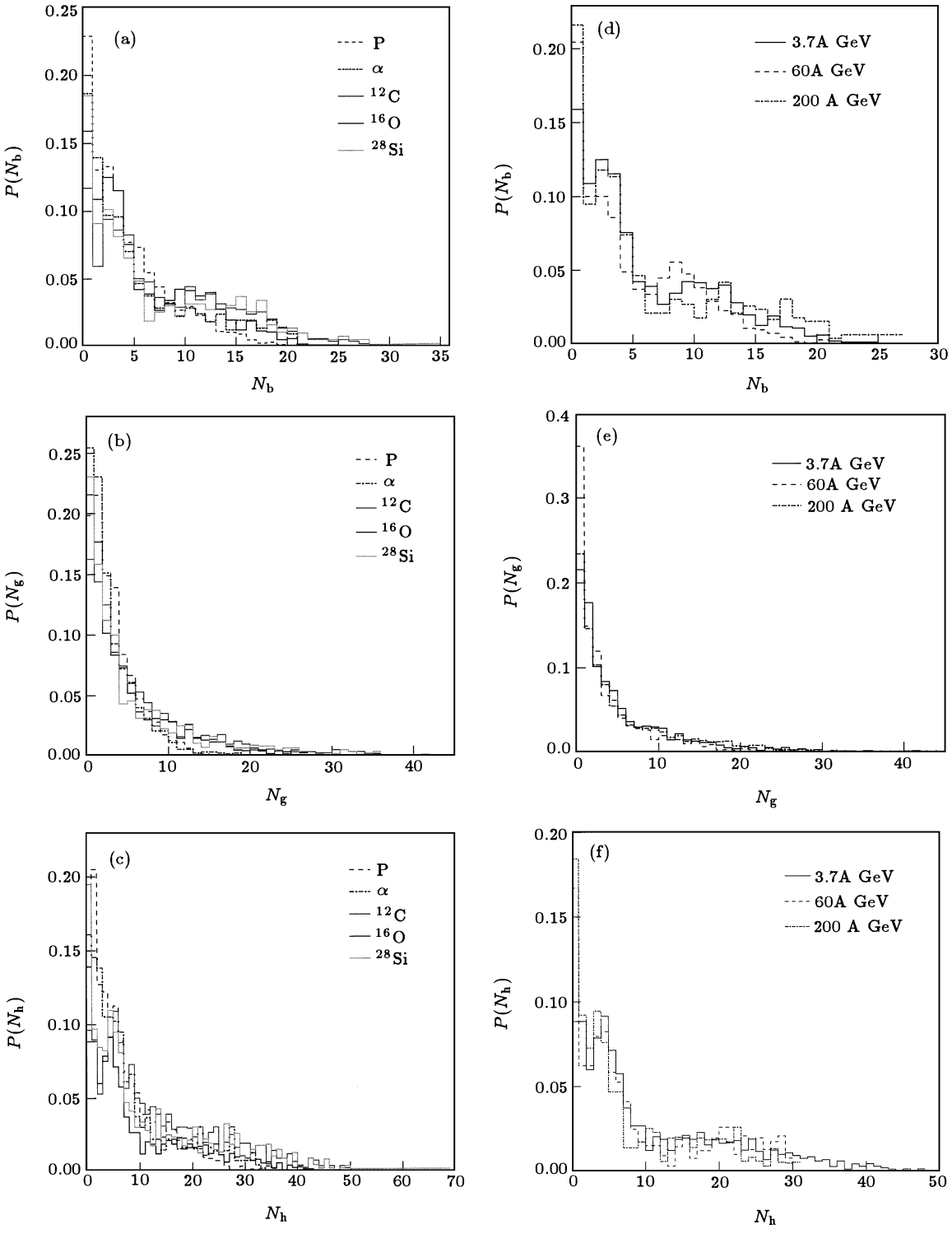


Fig.1. Multiplicity distributions of slow particles for ^{16}O–Em interactions at different energies and p–Em, α–Em, ^{12}C–Em, and ^{28}Si–Em interactions at 4.5 A GeV/c. (a) and (d) N_b distribution; (b) and (e) N_g distribution; (c) and (f) N_h distribution.

(2) For different projectiles at the same energy, the distributions are essentially similar. However, it is noticed from the figure that the percentage of events with lower values of N_g, N_b, or N_h decreases with the increase in projectile mass, or conversely, the percentage of events with large values of these parameters increases with the projectile mass.

Figure 2 shows the multiplicity distribution of grey, black and heavy particles emitted from 3.7 A GeV ^{16}O–Em interactions and the corresponding results from FRITIOF (version 1.7). Since no significant differences are observed regarding the slow particle production, in the FRITIOF model calculations we use an incident energy of 200 A GeV. From these figures we find a good agreement between the data and the model, although the model calculations exhibit a somewhat larger tail. The tendency of a bump in the region around $N_b = 10$ and $N_h = 15$ seen in the data is not reproduced by the calculations.

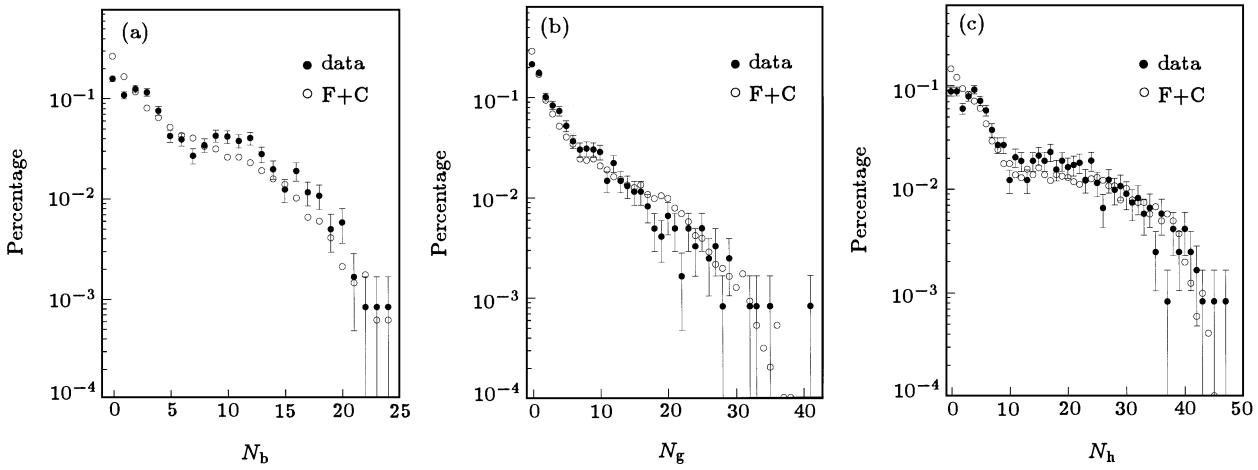


Fig.2. Multiplicity distributions of slow particles for ^{16}O–Em interactions at 4.5 A GeV/c and the corresponding results from FRITIOF 1.7 prediction. (a) N_b-distribution; (b) N_g-distribution; (c) N_h-distribution.

Table 3. The mean multiplicity of slow particles for different types of ^{16}O–Em interactions.

Type of events	$< N_b >$	$< N_g >$	$< N_h >$
peripheral event	3.87 ± 0.14	2.71 ± 0.13	6.59 ± 0.24
minimum bias event	5.38 ± 0.15	4.80 ± 0.17	10.18 ± 0.29
central event	8.46 ± 0.28	9.06 ± 0.36	17.52 ± 0.57

Table 3 presents the mean multiplicity of black, grey and heavy particles in minimum bias events, peripheral and central events of ^{16}O–Em interactions at 4.5 A GeV/c. It is found that the mean multiplicity of slow particles increases with the increase of the centrality of collision. In Fig.3 we present the multiplicity distribution of slow particles in ^{16}O–Em central interactions. Again it is found that N_b distribution is composed of two parts $N_b \leq 6$ and $N_b \geq 7$ which correspond to the contributions of light target (CNO) and heavy target (AgBr) of the emulsion respectively, while the N_h distribution is composed of two parts $N_h \leq 8$ and $N_h > 8$ which can be well explained by the contributions of light and heavy targets of the emulsion.

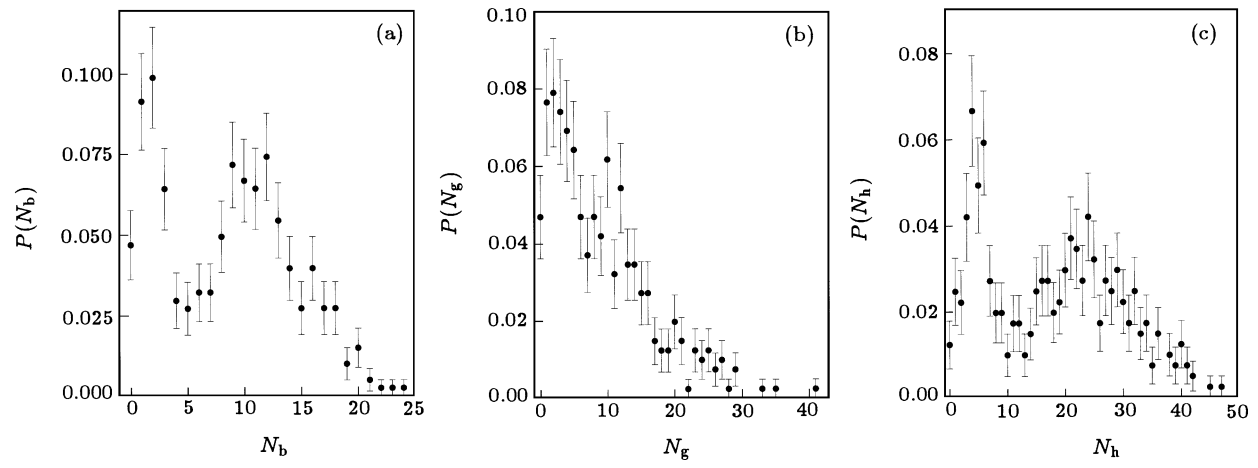


Fig.3. Multiplicity distributions of slow particles for central ^{16}O–Em interactions at 4.5 A GeV/c. (a) N_b-distribution; (b) N_g-distribution; (c) N_h-distribution.

3.3. Correlations of slow particles

We have also studied the correlations among different multiplicity parameters with a view to ascertaining a continuity from the p–nucleus to nucleus–nucleus interaction mechanism. Figure 4 shows the dependence of $< N_i >$ on N_j, where $i \neq j$ means b, g, s and h. Generally, the experimental results have been analysed by using linear fits of the type

$$< N_i(N_j) >= a_{ij} N_j + b_{ij}. \quad (1)$$

The values of a_{ij} and b_{ij} obtained by the least-square fitting for ^{16}O–Em interactions are listed in Table 4. For comparison, the correlation coefficient a_{ij} for different projectiles induced nuclear emulsion interactions at 4.5 A GeV/c is presented in Table 5. The following conclusions may be drawn from the results of Fig.4 and Tables 4 and 5:

(1) Variation of $< N_s >$ with N_b, N_g and N_h. It is observed that $< N_s >$ increases with the increase of N_b, N_g and N_h in the case of ^{16}O–Em collisions and also other nucleus-induced emulsion interactions; however, in p–Em interactions negative correlation is observed.

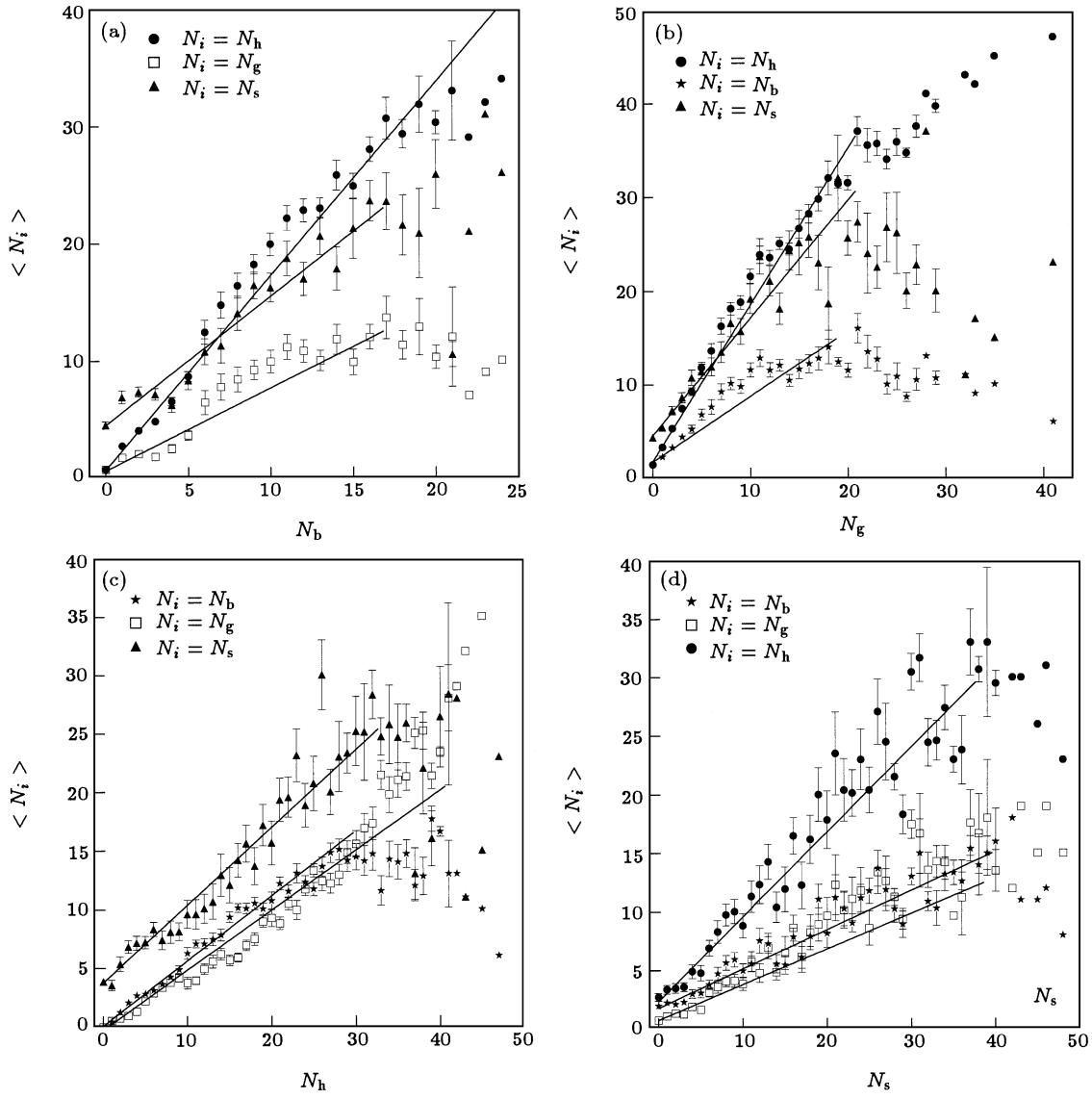


Fig.4. Multiplicity correlations of type $< N_i(N_j) >$ with $i \neq j$ in ^{16}O–Em interactions at 4.5 A GeV/c.

(2) Variation of $< N_b >$ with N_s and N_g. Very clear saturation in the values of $< N_b >$ is observed in $< N_b >$ versus N_g plot for values of N_g beyond ~ 10. A similar result was obtained by Otterlund [27] for p–nucleus interactions over a wide range of energy. This means that the correlation does not depend on the mass of the projectile, and the contribution of the recoiling nucleons towards the excitation energy of the residual nucleus is approximately the same for p–nucleus and nucleus–nucleus interactions. $< N_b >$ decreases with the increase of N_s in proton–nucleus collisions and it increases with the increase of N_s in nucleus–nucleus interactions.

(3) Variation of $< N_g >$ with N_s and N_b. The behaviour of $< N_g >$ variation with N_s or N_b is very similar to that of $< N_b >$ with N_s and N_g; however, the saturations are not statistically significant.

(4) $< N_g >$ displays a linear dependence on N_h in the whole range of N_h, but $< N_b >$ increases with the increase of N_h up to $N_h \sim 26$ and beyond this value of N_h, it gets saturation.

(5) $< N_h >$ increases with the increase of N_b, N_g and N_s in the whole range of N_b, N_g and N_s in nucleus–nucleus interactions but decreases with the increase of N_s in p–nucleus collisions.

Table 4. Values of the inclination coefficient, a_{ij}, and intercepts, b_{ij}, in the multiplicity correlations in ^{16}O–Em interactions at 4.5 A GeV/c.

	a_{ij}				b_{ij}			
N_j	$< N_b >$	$< N_g >$	$< N_h >$	$< N_s >$	$< N_b >$	$< N_g >$	$< N_h >$	$< N_s >$
N_g	$.70 \pm .02$		$1.67 \pm .01$	$1.25 \pm .04$	$1.80 \pm .09$		$1.84 \pm .09$	$4.57 \pm .19$
N_b		$.70 \pm .02$	$1.66 \pm .02$	$1.10 \pm .05$		$0.62 \pm .07$	$0.68 \pm .07$	$4.48 \pm .23$
N_h	$.55 \pm .01$	$.51 \pm .01$		$0.66 \pm .02$	$0.08 \pm .04$	$-0.27 \pm .04$		$3.74 \pm .16$
N_s	$.33 \pm .01$	$.30 \pm .01$	$0.72 \pm .01$		$1.79 \pm .12$	$0.76 \pm .08$	$2.33 \pm .17$	

Table 5. Values of the inclination coefficient a_{ij} in the multiplicity correlations in p–Em and nucleus-induced emulsion interactions at 4.5 A GeV/c.

Type of the		a_{ij}				Ref.
interaction	N_j	$< N_b >$	$< N_g >$	$< N_h >$	$< N_s >$	
p-Em	N_b		0.47 ± 0.02	1.46 ± 0.02	$-0.03 \pm .01$	[18]
^{12}C-Em	N_b		0.59 ± 0.04	1.60 ± 0.04	0.47 ± 0.04	[18]
^{16}O-Em	N_b		0.70 ± 0.02	1.66 ± 0.02	1.10 ± 0.05	This work
^{28}Si-Em	N_b		0.62 ± 0.05	1.62 ± 0.05	1.14 ± 0.09	[18]
p-Em	N_g	0.99 ± 0.07		1.95 ± 0.05	$-0.05 \pm .01$	[18]
^{12}C-Em	N_g	0.98 ± 0.05		2.03 ± 0.04	0.71 ± 0.06	[18]
^{16}O-Em	N_g	0.70 ± 0.02		1.67 ± 0.01	1.25 ± 0.04	This work
^{28}Si-Em	N_g	1.27 ± 0.07		2.14 ± 0.07	1.87 ± 0.09	[18]
p-Em	N_h	0.61 ± 0.01	0.40 ± 0.01		$-0.02 \pm .01$	[18]
^{12}C-Em	N_h	0.57 ± 0.02	0.40 ± 0.01		0.35 ± 0.02	[18]
^{16}O-Em	N_h	0.55 ± 0.01	0.51 ± 0.01		0.66 ± 0.02	This work
^{28}Si-Em	N_h	0.63 ± 0.01	0.37 ± 0.01		0.70 ± 0.04	[18]
p-Em	N_s	$-0.04 \pm .20$	$-0.22 \pm .16$	$-0.28 \pm .24$		[18]
^{12}C-Em	N_s	0.78 ± 0.03	0.64 ± 0.03	1.29 ± 0.07		[18]
^{16}O-Em	N_s	0.33 ± 0.01	0.30 ± 0.01	0.72 ± 0.01		This work
^{28}Si-Em	N_s	0.39 ± 0.02	0.34 ± 0.01	0.69 ± 0.02		[18]

It is interesting to study the correlations of slow particles for different types of the ^{16}O–Em interactions. These studies can help us to understand the dependence of the nucleus–nucleus interaction mechanism on the interacting centrality. Figure 5 shows the dependence of mean multiplicity and dispersion of black particle on the number of grey particles for minimum bias events, central events and peripheral events of ^{16}O–Em interactions, where the dispersion is defined as $D(N_b) = \sqrt{< N_b^2 > - < N_b >^2}$. From the figure it is seen that $< N_b >$ and $D(N_b)$ have the same tendency for the three different types of interac-

tions. $< N_b >$ displays a linear dependence on N_g up to 10 and beyond this value of N_g, it gets saturation. $D(N_b)$ increases with the increase of N_g up to 6 and beyond this value of N_g, it also gets some saturation.

Figure 6 shows the dependence of $< N_g >$ and $D(N_g)$ on the number of black particles for minimum bias, central and peripheral events of ^{16}O–Em interactions. For minimum bias and peripheral events the same dependence is observed, $< N_g >$ and $D(N_g)$ increase with the increase of N_b, but for central interactions two distinct regions $N_b \leq 5$ and $N_b > 5$ are observed which correspond to the light target and heavy target regions of the emulsion. In each region, $< N_g >$ and $D(n_g)$ seems not to change too much.

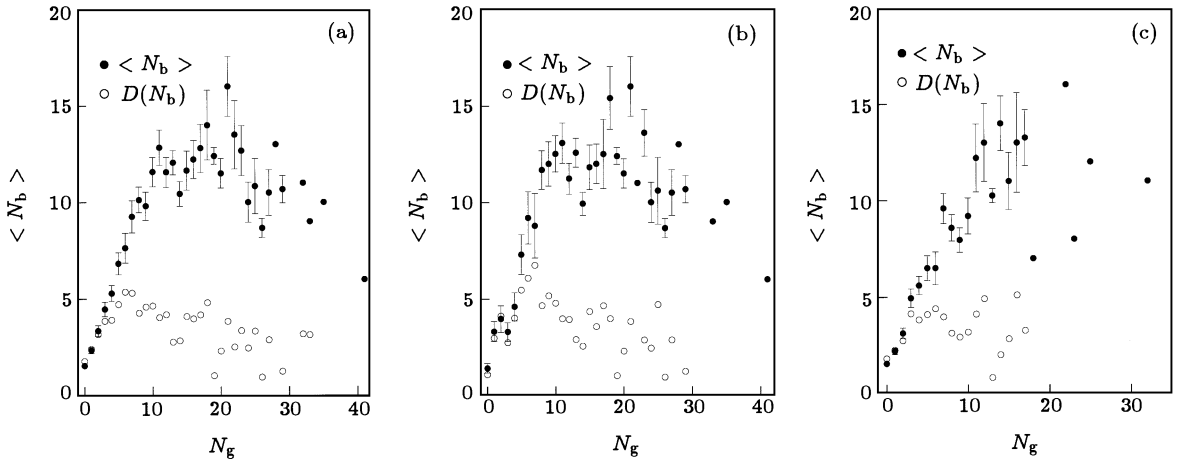


Fig.5. The dependence of $< N_b >$ and $D(N_b)$ on N_g for different types of ^{16}O–Em interactions at 4.5 A GeV/c. (a) minimum bias events; (b) central events; (c) peripheral events.

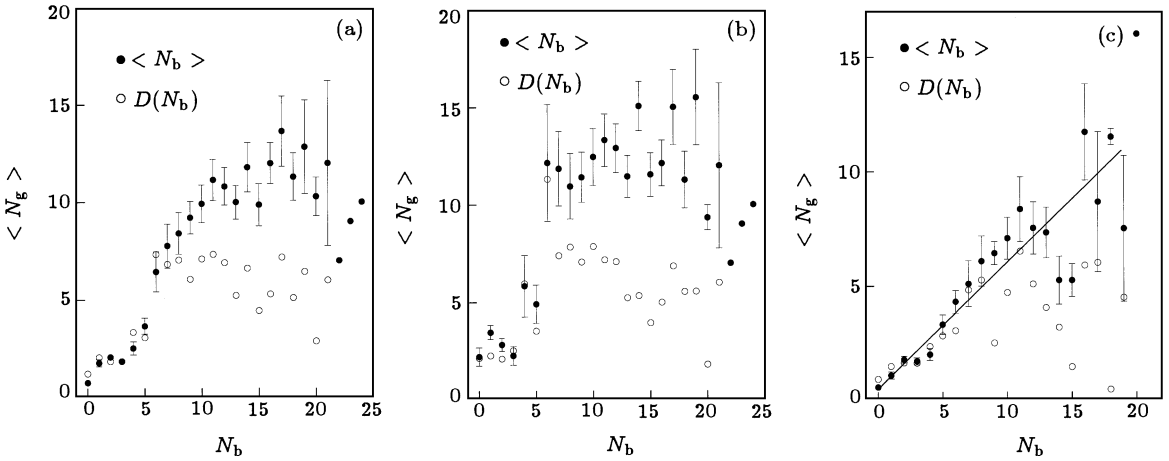


Fig.6. The dependence of $< N_g >$ and $D(N_g)$ on N_b for different types of ^{16}O–Em interactions at 4.5 A GeV/c. (a) minimum bias events; (b) central events; (c) peripheral events.

The dependence of $< N_h >$ on N_g, as shown in Fig.7, for minimum bias, central and peripheral interactions of ^{16}O–Em follows the same tendency; $< N_h >$ increases with the increase of N_g. Using formula $< N_h >= a(1 + N_g)^b$ to fit the experimental data we obtain

$$< N_h >=2.31(1 + N_g)^{0.85} \quad \text{(minimum bias events)}, \quad (2)$$

$$< N_h >= 2.97(1 + N_g)^{0.77} \quad \text{(central events)}, \quad (3)$$

$$< N_h >=1.76(1 + N_g)^{0.99} \text{(peripheral events)}. \quad (4)$$

From these fittings we can see that the parameter b increases with the decrease of collision centrality. For peripheral collisions the dependence of $< N_h >$ on N_g is almost linear (b=0.99), but for central collisions the linearity is decreased (b=0.77). These results can be well explained by the collision geometry.

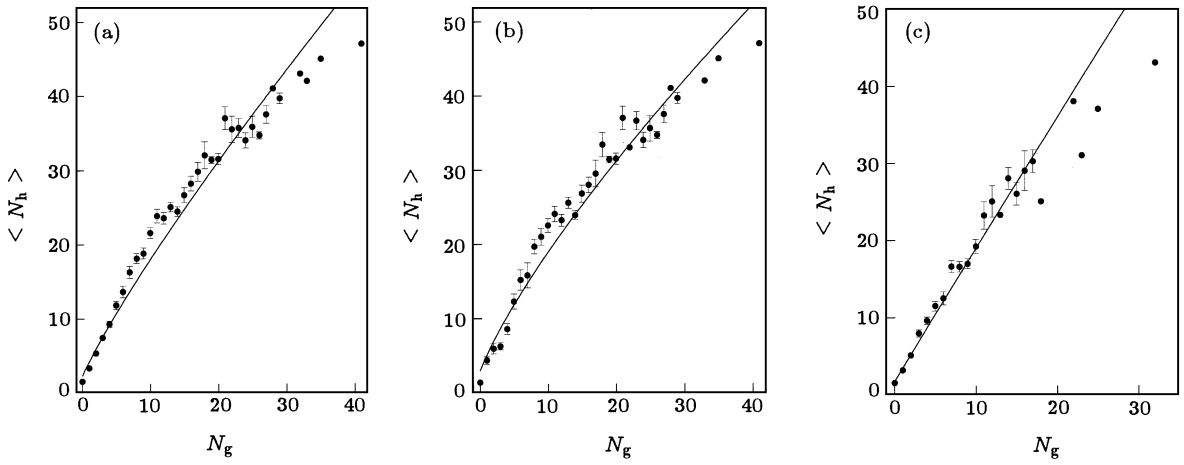


Fig.7. The dependence of $< N_h >$ on N_g for different types of ^{16}O–Em interactions at 4.5 A GeV/c. (a) minimum bias events; (b) central events; (c) peripheral events.

3.4. Angular distributions of slow particles

Figure 8 shows the angular distributions ($dN/d\theta$) for grey, black and heavy particles emitted from ^{16}O–Em collisions. Black particles, based on nuclear evaporation processes, are isotropically distributed in the rest frame of target nucleus, but the distribution is influenced by a strong electromagnetic field of relativistic projectiles, it is almost symmetric about $\theta \approx 90°$ in the laboratory system. Grey particles, based on intranuclear cascade processes, are mainly emitted in the forward direction. Table 6 presents the mean emission angle of the black and the grey particles emitted in ^{16}O–Em interactions and other nucleus-induced emulsion interactions at the same energy.

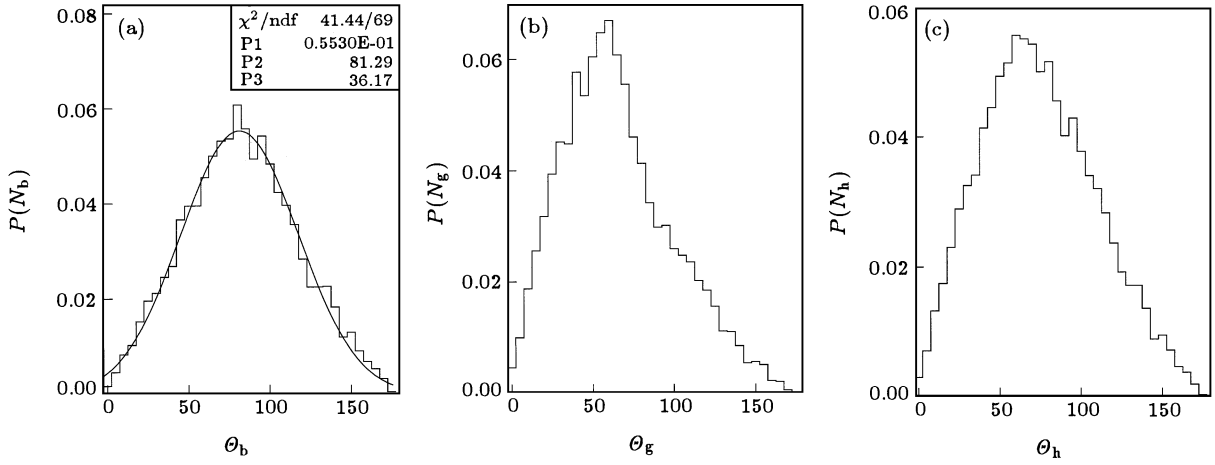


Fig.8. The angular distributions of slow particles for ^{16}O–Em interactions at 4.5 A GeV/c. (a) N_b-distribution; (b) N_g-distribution; (c) N_h-distribution.

Table 6. The mean emission angle of the grey and the black particles for different projectiles at 4.5 A GeV/c.

Projectile	$< \theta_b >$	$< \theta_g >$	Ref.
p	85.3 ± 1.9	68.0 ± 1.5	[28]
^{4}He	83.0 ± 3.8	62.8 ± 3.1	[28]
^{6}Li	82.2 ± 2.6	64.9 ± 2.2	[29]
^{12}C	79.5 ± 2.4	64.0 ± 1.9	[30]
^{16}O	85.0 ± 0.4	67.6 ± 0.4	This work

The angular distributions of grey and black particles emitted in ^{16}O–Em interactions at 4.5 A GeV/c and other nucleus-induced emulsion interactions at the same energy is shown in Fig.9. As can be seen from the figure, there is no dependence of these distributions on the mass of the projectile. It shows that the production mechanism of heavy particles is probably the same in p–nucleus and nucleus–nucleus interactions. It can also be seen that these distributions do not exhibit any peaks that could be attributed to the shock wave phenomenon.[31–34]

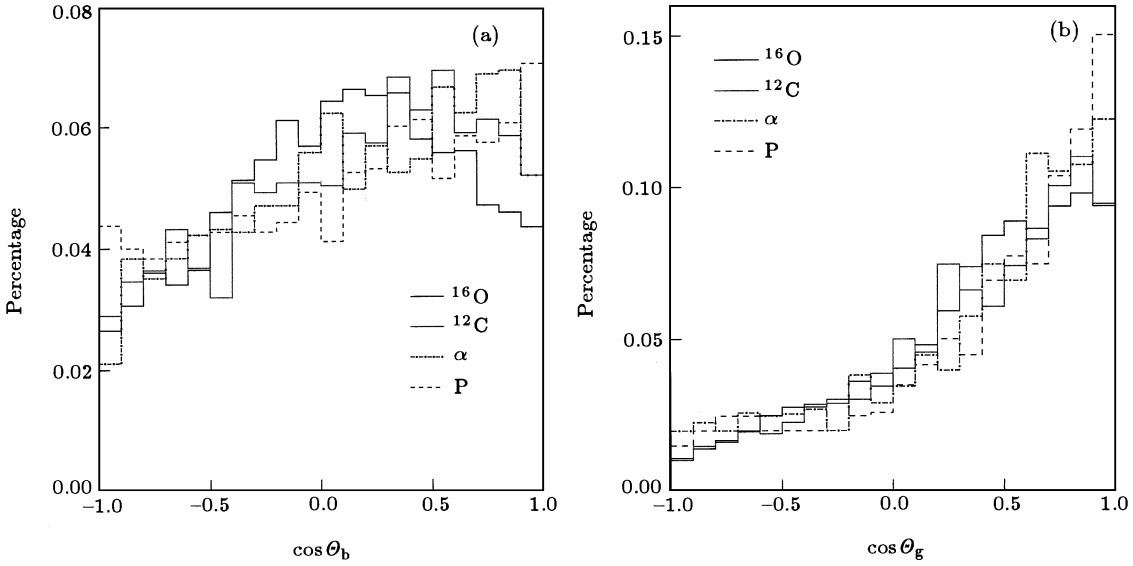


Fig.9. The angular distributions of slow particles for ^{16}O–Em interactions at 4.5 A GeV/c and other nucleus-induced emulsion interactions at the same energy. (a) N_b-distribution; (b) N_g-distribution.

4. Conclusions

From the analysis of ^{16}O–Em interactions at 4.5 A GeV/c we conclude that:

(1) The mean multiplicity of black particles does not depend on the mass of the projectile. However, the average multiplicity of grey particles depends on the mass of the projectile.

(2) The dependence of $< N_b >$ on N_g in ^{16}O–Em interactions is almost the same as in p–nucleus interactions.

(3) The correlations of slow particles in nucleus-induced emulsion interactions at 4.5 A GeV/c have the same tendency for different projectiles.

(4) The angular distribution of slow particles emitted in nucleus-induced emulsion interactions is independent of the projectile energy and mass.

(5) The results of slow particles production in ^{16}O–Em can be described in terms of the participant and spectator model.

Acknowledgment

We are grateful to Professor I. Otterlund of Lund University in Sweden for supplying the emulsion plates.

References

[1] Lee T D 1975 *Rev. Mod. Phys.* **47** 267
[2] Glassgold A E *et al* 1959 *Ann. Phys.* **6** 1
[3] Boguta J 1982 *Phys. Lett.* B **109** 251
[4] Kapusta J 1979 *Nucl. Phys.* B **148** 461
[5] Adamovich M I *et al* 1995 *Z. Phys.* C **65** 421
[6] Andersson B, Otterlund I and Stenlund E 1978 *Phys. Lett.* B **73** 343
[7] Stenlund E and Otterlund I 1982 *Nucl. Phys.* B **198** 407
[8] Barkas W H 1963 *Nuclear Research Emulsion* 1st edn. (New York: Academic) 349
[9] Goldhaber A S 1974 *Phys. Lett.* B **53** 306
[10] A-ABDDKLMTU-B Collaboration 1981 *Z. Phys.* A **302** 133
[11] DGKLMTW Collaboration 1974 *JINR Dubna Commun.* pp1–8313
[12] Ahmad T 1991 *Ph.D. Thesis,* Aligarh Muslim University, Aligarh, India
[13] Ahmad T, Nasr M A and Irfan M 1993 *Mod. Phys. Lett.* A **8** 1103
[14] Ghosh D, Mukhhopadhya A, Ghosh A and Sengupta R 1989 *Nucl. Phys.* A **499** 850
[15] Sherif M M, Hegab M K, El-Sharkawy S and Tawfik A M 1993 *Proc. 1st Int. Conf. on Engineering Mathematics and Physics (Cairo)* p1459
[16] Khan M Q R, Ahmad M S, Siddiqui K A and Hasan R 1988 *Nuovo Cimento Soc. Ital. Fis.* A **99** 417
[17] Khan M S, Khushnood H and Ansari A R 1996 *Can. J. Phys.* **74** 651
[18] Tariq M, Zafar M, Tufail A and Ahmad S 1995 *Int. J. Mod. Phys.* E **4** 347
[19] Heckman H H, Greiner D E, Lindstrom P J *et al* 1978 *Phys. Rev.* C **1978** 1735
[20] Bannik B P *et al* 1984 *Sov. J. Nucl. Phys.* **52** 982
[21] El-Sharkawy S, Hegab M K, Osman O M and Jilany M A 1993 *Phys. Scripta* **47** 512

[22] Jilany M A, Abd Allah N N and Abd Eldaim A 1995 *Int. J. Mod. Phys.* E **4** 815
[23] Nasr M A and Khushnood H 1994 *Int. J. Mod. Phys.* A **9** 5145
[24] Jilany M A 1994 *Nucl. Phys.* A **579** 627
[25] El-Nadi M, Mettwalli N, Shaat E A *et al* 1996 *Int. J. Mod. Phys.* E **5** 617
[26] Ardito N *et al* 1988 *Europhys. Lett.* **6** 131
[27] Otterlund I 1978 *Preprint* LUIP-7804 Lund University
[28] ABGDDEKKLMRTTV Collaboration 1987 *Sov. J. Nucl. Phys.* **45** 78
[29] Sherif M M, Hegab M K and Abdelsalam A 1993 *Int. J. Mod. Phys.* E **2** 835
[30] BWDKLMT Collaboration 1979 *Sov. J. Nucl. Phys.* **29** 52
[31] Baumgardt H G, Schott J U, Sakamoto Y *et al* 1975 *Z. Phys.* A **273** 359
[32] Heckmann H H, Karant Y J and Friedlander E M 1986 *Phys. Rev.* C **34** 1333
[33] Jakobsson B, Kullberg R and Otterlund I 1977 *Nucl. Phys.* A **276** 523
[34] Ghosh D, Roy J and Sengupta R 1986 *Can. J. Phys.* **64** 1502